Patterns on Desert Plants

Alan C. Newell, Department of Mathematics, The University of Arizona, Tucson, Arizona, anewell@math.arizona.edu

Patrick D. Shipman, Department of Mathematics, Colorado State University, Fort Collins, Colorado, shipman@math.colostate.edu

Todd J. Cooke, Department of Cell Biology and Molecular Genetics, University of Maryland, College Park, Maryland tjcooke@umd.edu

Abstract

The patterns seen in both the phyllotaxis and surface morphologies in the vicinity of the shoot apical meristems of plants are discussed. We begin with many pictures and a narrative descriptive of both the universal and anomalous features of desert and other plants. We then briefly outline explanations and open challenges. Although many of the special features of phyllotaxis have been known for over four centuries, only now are mechanistic explanations beginning to emerge.

Descriptive Narrative

Consider the collage of desert plants, a pine cone, and sunflowers in Fig. 1 and throughout this article. These plant structures display obvious arrangements of their parts, which arise from the activity of the plant growth center called the shoot apical meristem (SAM). We observe patterns both in the positioning of the phylla (the areolae (short shoots bearing spines) on cacti, ovuliferous scales on pine cones, flowers and fruitlets (colloquially called seeds) on sunflowers) as well as in the morphology of the plant surface. Also note that the pattern exhibited by the cactus of Fig. 2 can be described in two ways. On the one hand, there is the tiling of the plant surface into irregular hexagons, as marked by the black lines in Fig. 2 (b,d). On the other hand, the plant's areoles are arranged in three families of spirals as marked by white lines in Fig. 2 (b,d) – families of five (three) spirals emanate (counter) clockwise from the plant center and intersect a family of eight (= 3+5) purely radial "spirals." These two descriptions of the pattern are, in fact, dual to each other: each areole lies in the center of a hexagonal region (in fact, at a local maximum of the surface) and at the intersection of three spirals, whereas any spiral is transverse to opposite sides of hexagons. This first example demonstrates what is commonly referred to as "spiral phyllotaxis" – phylla (leaves, or bracts of a pine cone, florets of a flower, or, as in this example, areolae on a cactus) are arranged (taxis) in spirals. The numbers (3,5,8) of spirals in this example are consecutive members of the regular Fibonacci sequence (1, 1, 2, 3, 5, 8 ...). One forms the regular Fibonacci sequence by starting with the initial term (1,1) and then applying the simple algorithm of finding the next member m_{j+1} of the sequence by adding the previous two ($m_{j+1} = m_{j-1} + m_j$). The prevalence of regular Fibonacci numbers in spiral phyllotaxis has long been noted. The first recorded observation is due to Johannes Kepler. An example of Fibonacci-spiral phyllotaxis with families of 8 counterclockwise and 13 clockwise spirals appears in Fig. 3. According to the data of (11, 20) (which does not include cacti), 92% of plants with spiral phyllotaxis exhibit the Fibonacci sequence. In the other cases, Fibonacci-like sequences, employing different initial terms but the same generating algorithm, such as the double Fibonacci sequence (2,2,4,6,10 ...) or the Lucas sequence (1, 3, 4, 7, 11...) appear.

You can test your spiral-counting ability on the plants shown in Fig. 1. Try the sunflower! If you perform this exercise and count the numbers of spirals in cacti that you see on desert walks, you might come to question the stated ubiquity of the regular Fibonacci sequence. Indeed, although the regular Fibonacci sequence does appear on cacti, it is not hard to find cacti with spiral phyllotaxis belonging to many other Fibonacci-like sequences. In this article, we describe how unusual features of cacti and desert plants led us to study phyllotactic patterns on plants, how phyllotactic patterns are related to other patterns in nature, and how the phyllotaxis of cacti might inform the study of how these patterns form.

First, we describe the other common class of phyllotactic patterns. One observes hexagons also on the cactus of Fig. 4, a larger specimen of the same species as the cactus of Fig. 4. Dual to this hexagonal tiling, there are also families of spirals – in this case, a family of six clockwise spirals and a family of six counterclockwise spirals intersect at the areoles of the plant with a family of twelve (= 6+6) purely radial spirals. This results in an arrangement of areoles which places groups of six areoles equally spaced about a circle centered at the plant tip. Each whorl of six areoles is shifted circumferentially from neighboring whorls by an angle of $\pi/6$. This example thus demonstrates what is referred to as an alternating whorl pattern. We will call it an alternating 6-whorl. The most commonly observed whorl pattern in nature is the decussate pattern seen in the succulent and cactus of Fig. 5; notice pairs (2-whorls) of phylla alternating in angle. An N-whorl will have N phylla at the same radius as measured from the SAM center. A regular Fibonacci spiral pattern will only have one at certain radii.

Although both of the plants in Fig. 5 follow decusate phyllotaxis, ridges dominate on the cactus of Fig. 5(b), whereas the phylla of the succulent of Fig. 5(a) dominate as individual entities. This aspect of plant patterns – that similar phyllotactic arrangements associate with very different surface morphologies – has been largely ignored in studies of phyllotaxis, although Williams points to this in a set of beautiful drawings of plant meristems [45]. But, it is impossible to study the patterns on (desert) plants without noticing a variety of surface morphologies ranging from those dominated by ridges, to hexagonal planforms, to other tilings. In Fig. 6(a) one sees the radial ridges on a pumpkin; in this example, there are no phylla to be arranged along the ridges. In fact, there are no equivalents to phylla visible on pumpkins. The underlying reason for their patterns is still open. The saguaro cactus of Fig. 6(b) is also strongly ribbed; in this case, however, areoles are arranged along the ridges in (if there are an even number of ridges) an alternating whorl pattern. Ridges are also dominant in the cacti of Fig.6 (c,d); in these cases, there are Fibonacci numbers of ridges and the areoles are arranged in families of Fibonacci numbers of spirals. The figure concludes with more examples of hexagonal planforms on plants – on a pine cone (Fig. 6(e), a cactus (Fig. 6(f)) and on the trunk of an elephant tree (Fig. 6(g)). Ridges and hexagons are often observed on different examples of the same species, as in the totem pole cactus of Fig. 7 or on the same plant as in Fig. 8. There are also other polygonal patterns seen on plants; for example, although hexagons are seen on the cactus of Fig. 9(a), it is rhombi that are seen on the cactus of the same species in Fig. 9(b). Fig. 10 gives a summary of a range of tiling morphologies.

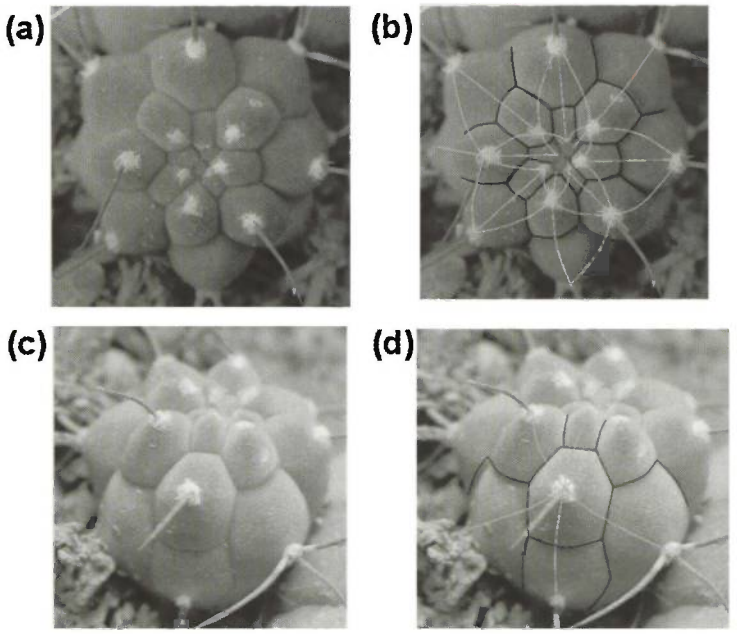

Figure 2. An irregular-hexagonal tiling and Fibonacci spirals on a cactus of the genus *Matucana*.

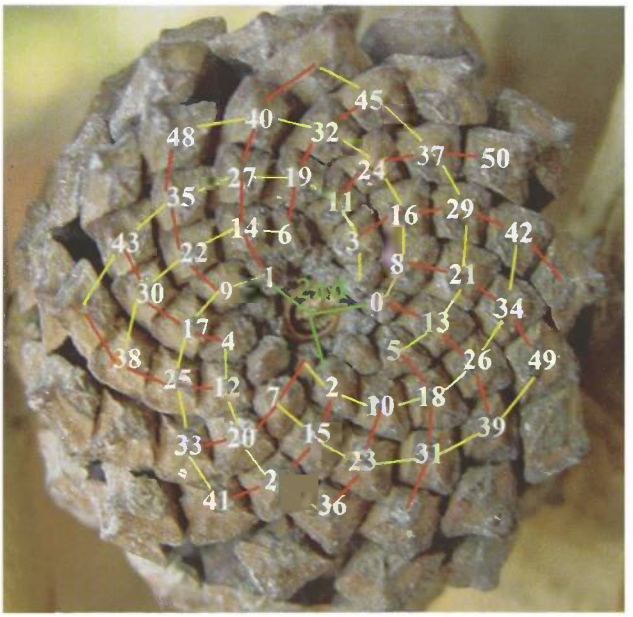

Figure 3. Fibonacci spirals on a pinecone.

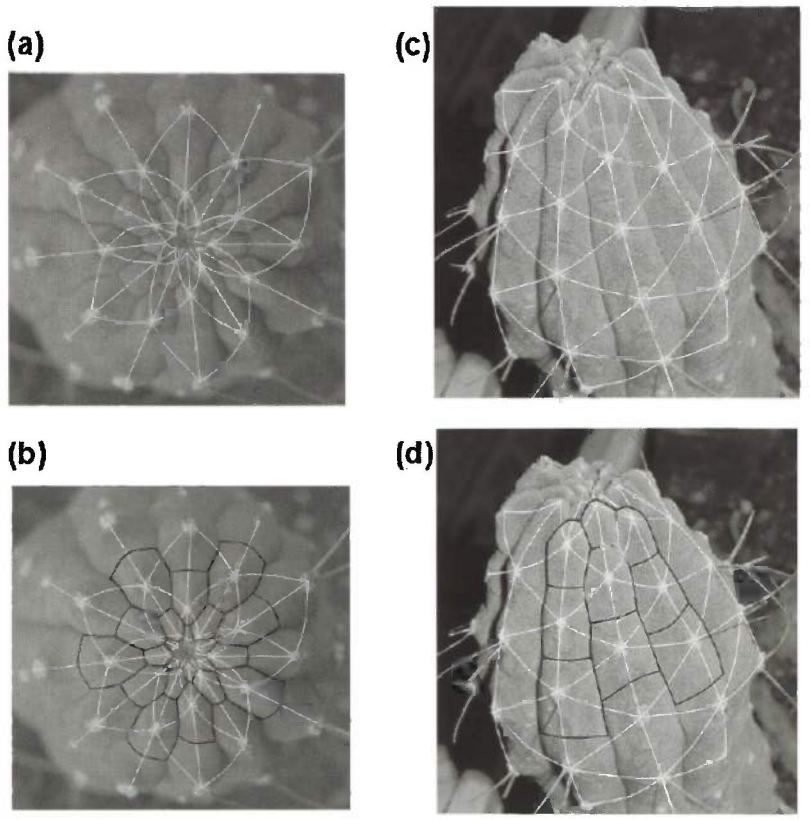

Figure 4. An irregular-hexagonal tiling and 6-whorl phyllotactics on a cactus of the genus *Matucana*.

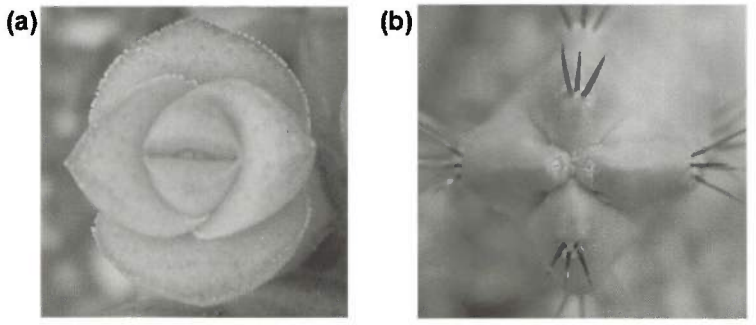

Figure 5. The decussate (alternating 2-whorl) phyllotactic pattern. Phylla form in opposite pairs that alternate in at right angles to each other.

Often, different regions of a single plant show different patterns, and the different configurations are mediated by defects. In Fig. 11, dislocations (where a ridge ends or forks) separate regions with different numbers of ridges around saguaro cacti (the number of ribs increases moving towards the top). Dislocations are also seen in the Arizona Barrel cactus of Fig. 12 which is making a transition from a pattern with 13 ribs to one with 7 more ribs (one more new rib will appear later, making for a total of 8 new ribs!). Look at the saguaro or the barrel cactus. The number of ribs separated by the dislocation defect always increases away from the plant shoot. Why? The number of ribs is determined by the number of "unstable wavelengths" which can fit around the annulus at which they are generated. The radius of this annulus increases as the plant grows so that there are always more ribs near the top (near the shoot apical meristem) than the bottom. Look at the sunflower in Fig. 1(c). On the outside the spiral families contain 55 and 34 spirals, respectively, and the seeds fall in a rhombic pattern. On the inside, the families have 34 and 21 spirals, and again the pattern of seeds is more or less rhombic. In the transition zone, observe that the pattern undergoes a transition from 55/34 rhombi to the 34/21 rhombi with hexagonal structures.

Explanations

The questions which have challenged scientists since the time of Kepler are: Why do the phylla of plants tend to be arranged in spiral and whorl patterns?

In spiral arrangements, why are Fibonacci numbers so ubiquitous?

Considering the huge advances which have been made in the natural sciences over the past two hundred years, it is rather astonishing that answers to these, and deeper questions have only begun to emerge in the last decade or so. The deeper questions include: What is the mechanism behind the formation of primordia?

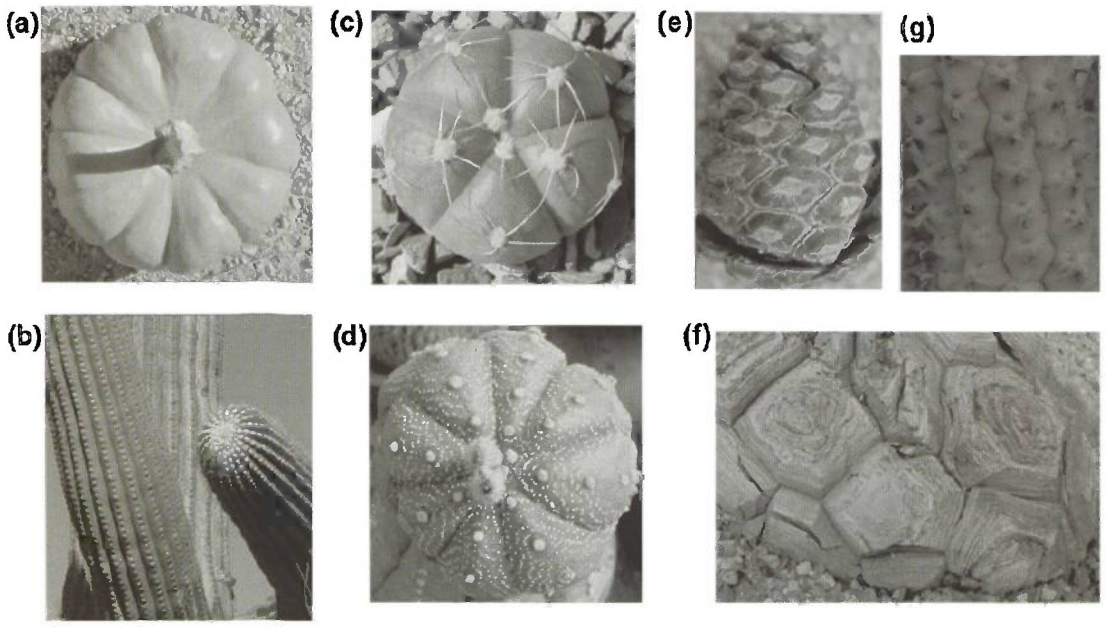

Figure 6. (a) Pumpkins do not have phylla, but they do have ridges. (b) Saguaro cacti have ridges, but also areoles arranged along the ridges. (c,d) These cacti have Fibonacci numbers of ridges and areoles arranged along the ridges. Hexagons are apparent on this (e) pinecone, (f) elephant tree trunk, and (g) succulent.

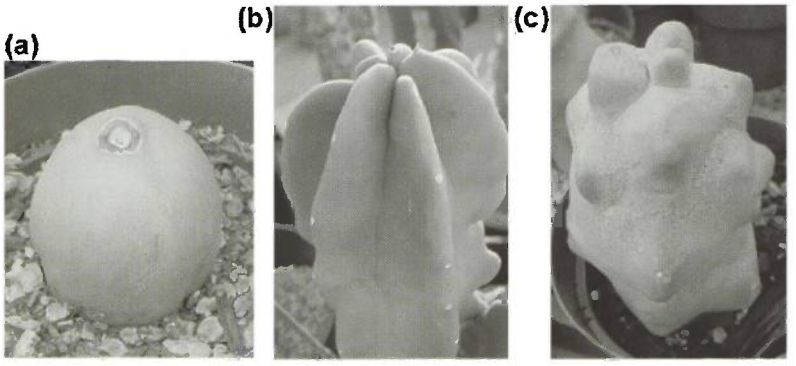

Figure 7. Totem pole cacti showing (a) no deformation from a spherical shape, (b) ridges, and (c) hexagons.

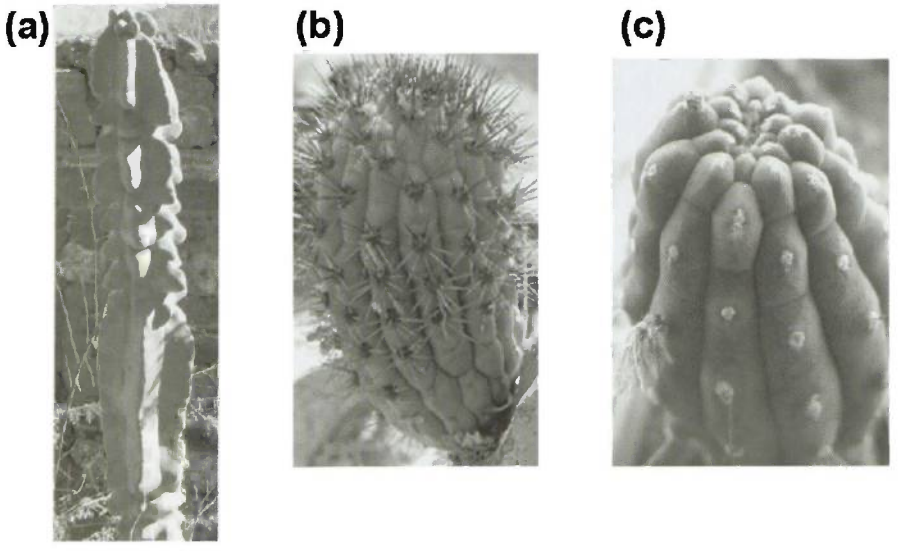

Figure 8. Ridges and hexagons on (a) totem pole cactus, (b) organ pipe cactus, and (c) a cactus of the genus *Matacana*.

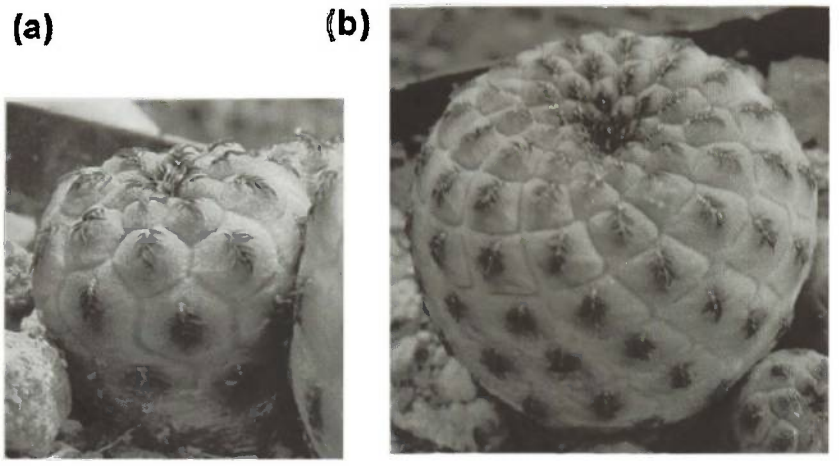

Figure 9. (a) Hexagons and (b) rhombi on these *Sulcorebutia rauschii* cacti.

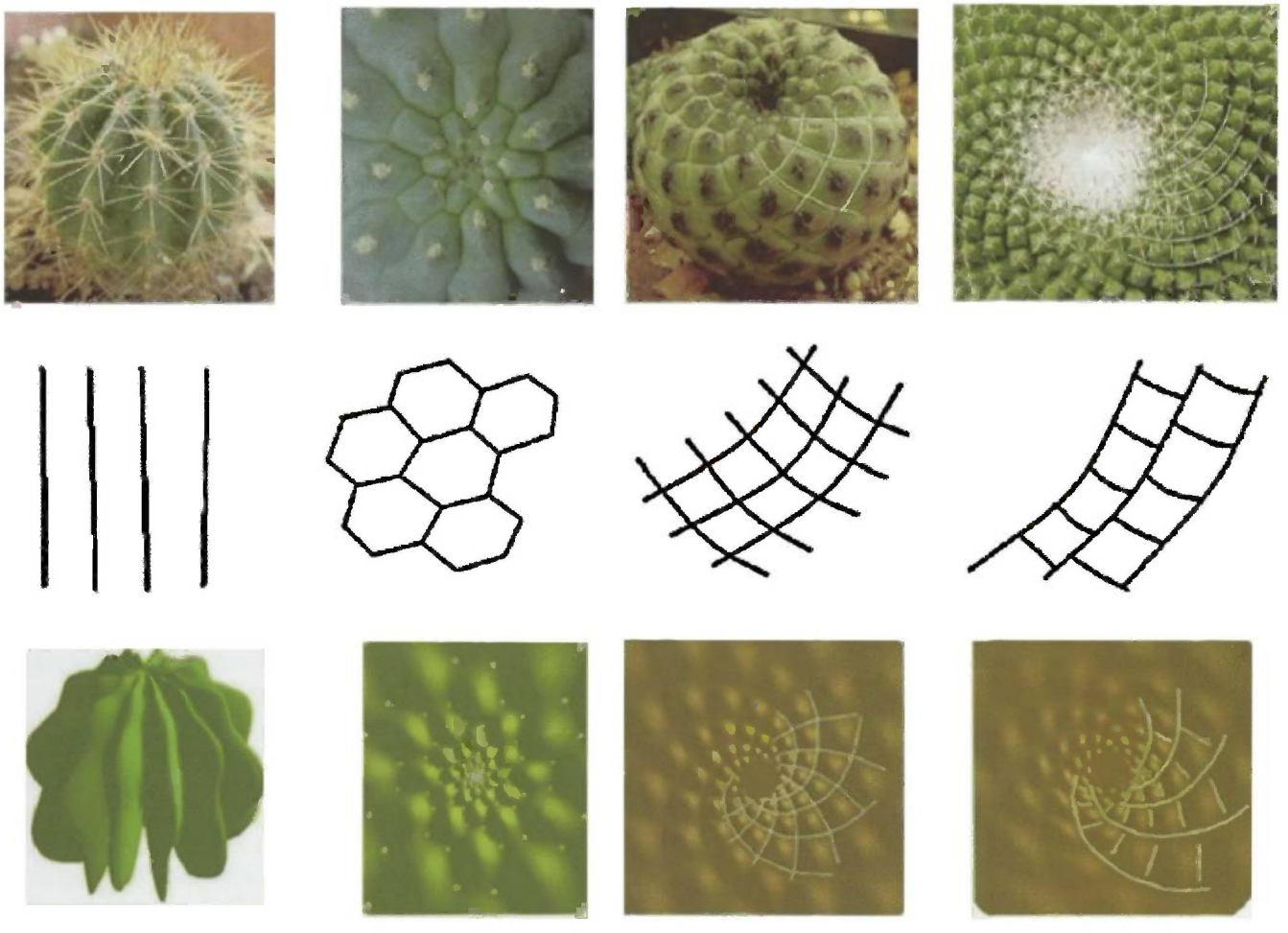

Figure 10. Prototypical (a) ridge, (b) hexagonal, (c) rhombic, and (d) offset-rhombic planforms.

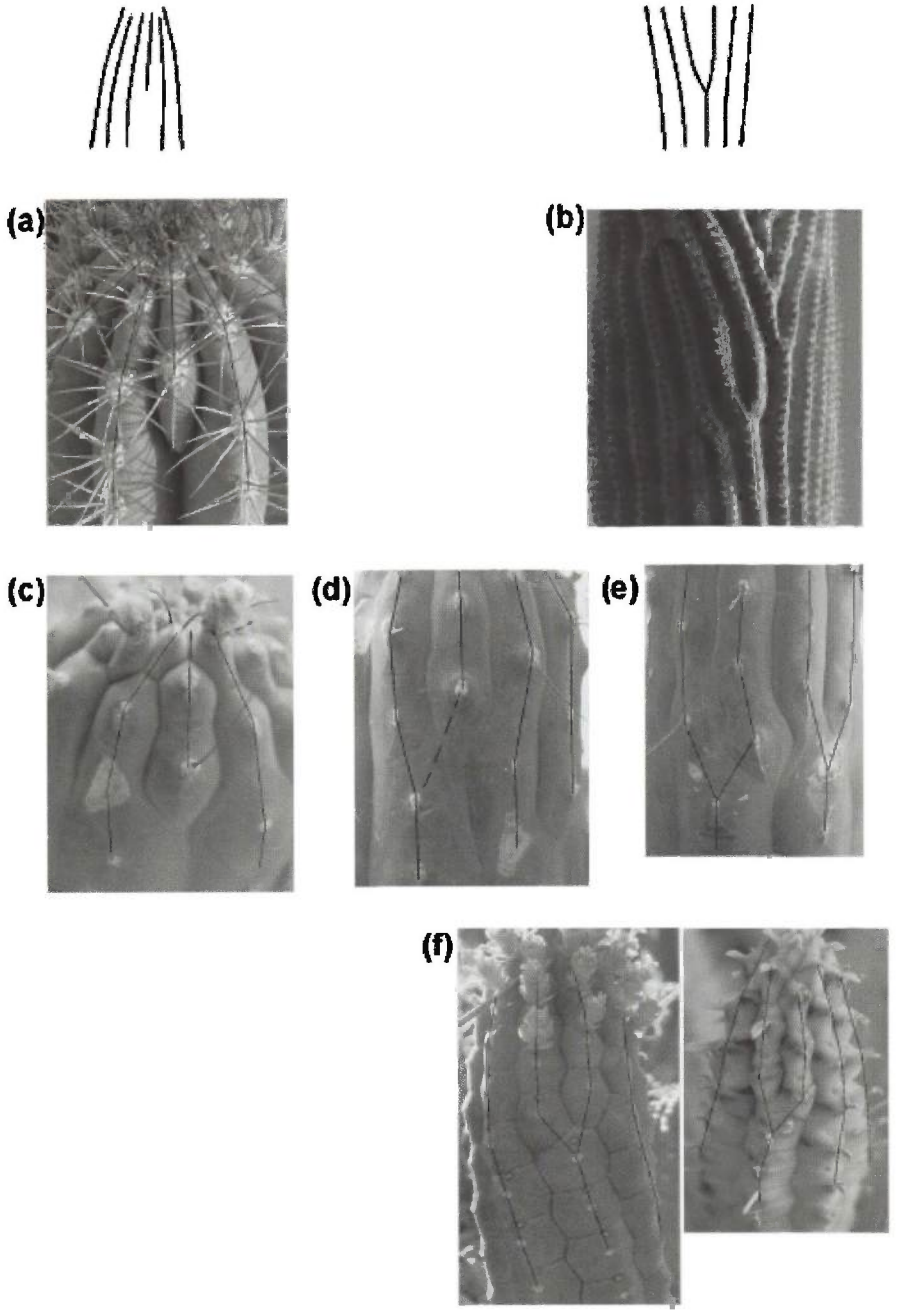

Figure 11. Dislocations in plant patterns. Ridges end or fork, forming dislocations.

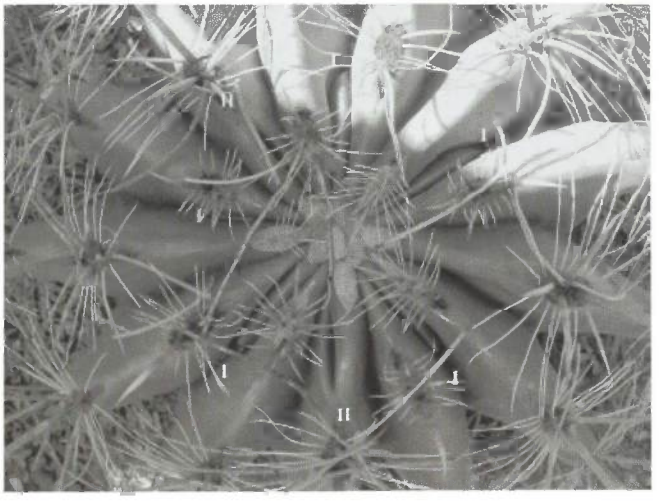

Figure 12. Dislocations on an Arizona barrel cactus.

Why do cacti often seem to grow in spurts, and what mechanisms would turn off and on growth?

And the question that has motivated much of our study of plant patterns is:
What determines the choice of planform ranging from ridges to hexagons to rhombi? In particular, why is it that, particularly on desert plants, the surface deformations are often dominated by distinct ridge-line structures (such as those on saguaro cacti and barrel cacti), even as the areoles also lie on spirals? We give a possible explanation later in this article.

Explanations for plant patterns have focused on the questions of the reasons for the prevalence of the Fibonacci sequences and the mechanisms behind primordium foundation. They fall into two categories. The first category we label descriptive and teleological; the second we call mechanistic. Hofmeister [18] and then Snow and Snow [40] were among the first to seek a prescriptive means for the positioning of phylla near the shoot apical meristem. Based largely on observations and empirical evidence, their efforts gave rise to the hypotheses that new primordia are initiated in the first available space (Hofmeister) or the place where there is least influence from existing primordial (Snow and Snow). Their rules were recast in algorithms which appealed to the idea that new phylla form in the "most open space" available and were supported by experiments using repelling ferromagnetic droplets (Douady and Couder [7]) and by looking for minimum energy configurations of vortices in superconducting materials (Levitov [26]. They gave rise to the teleological notion (X is so in order that the outcome Y is achieved) that somehow the plant has an inbuilt algorithm to position the phylla for some maximal advantage. But such arguments only beg the next question.

How does the plant actually know what to do? Algorithms which express many of these ideas have been turned into simulations and are reflected in the works of van Iterson [44], Douady and Couder, and Levitov and most recently of Atela, Gole and Hotton [1]. Indeed, the algorithm based on the Hofmeister rules leads naturally to phylla sets displaying Fibonacci spirals and to many of the intriguing self-similar properties which are observed. The rules of Snow and Snow were slightly less rigid than those of Hofmeister and allowed for whorl as well as spiral patterns. The phyllotactic patterns on ridge-dominated cacti are unusual, however, in that on close examination one finds that they do not quite obey the "most open space" rule. Indeed, many cacti undergo transitions from N-whorls to (N, N+1, 2N+1) spirals, and then to (N+1)-whorls (that is, for example, from the deccusate pattern/2-whorls to a (2,3,5)-spiral pattern, to 3-whorls). At the spiral stage, the Hofmeister rule is violated. Cacti actually construct their whorls in a very different fashion from other plants with whorls of three of more equivalent independent primordia, such as the horsetail Equisteum or the aquatic angiosperms. In these plants, the transition between adjacent whorls with different numbers of primordia are direct without any intervening spiral transitions Bierhorst [3] and McCully *et al.* [27]. The situation is different in whorl-mimics that split their primordia to form multiple primordial or recruit other leaf parts such as stipules to form leaf-like structures Kelly and Cooke [22]. The ability of the cacti to switch back-and-forth between whorls and spiral give them the potential to become very informative experimental systems for studying phyllotactic mechanisms.

Mechanistic (efficient) explanations, on the other hand, attempt to answer the question of how it is that the observed patterns are generated, namely, which biochemical and physical processes are the means through which the observed morphologies actually emerge and lead to the observed pattern formations. It is this approach that we have followed in our explanation attempts, and it has also been the preferred viewpoint of recent work by the groups of Kuhlemeier [10, 32, 33, 39] and Meyerowitz [21, 16, 14] on how transport of the growth hormone auxin can lead to phyllotactic patterns, as well as earlier work of Green and colleagues [12, 41, 8, 17] who proposed a biophysical mechanism for the formation of primordia, whereby compressive stresses due to growth lead to a buckling of the tunica (the outer layer of the plant). Before briefly describing this approach, we remark on a fascinating result which we have recently reported: *The two approaches lead to outcomes which are strikingly similar (Shipmand et al. [38]), at least for arrangement of primordia in spiral phyllotaxis. In other words, the mathematics which captures the tunica buckling and auxin-driven mechanistic models leads to the prediction of auxin concentration and surface deformation fields whose maxima closely mirror the set of phylla positions dictated by the algorithms of most open space.* Indeed, as d'Arcy Thompson noted in his celebrated masterpiece On Growth and Form (Thompson [42]), "like warp and woof, mechanism and teleology are interwoven together."

The mechanism-based explanation is motivated by the ubiquitous appearance of regular patterns in both nature and laboratories. For example, stripes with very similar features are observed on sand dunes, on fingerprints, on animal coats, and on fish skins (Boyle [19]). Both stripe and hexagonal planforms are seen in experiments on fluid convection, on compressed elastic sheets, in the mixing of chemical morphogens, on counter-propagating light beams, in geological formations, as granular cells on the surface of the sun, and in nanoscale structures produced by bombarding silicon surfaces by ions. Such patterns arise as instabilities when systems undergo some kind of external stress, such as the negative temperature gradient in a layer of fluid heated from below. At a certain threshold value of this stress, the uniform state becomes unstable, and certain shapes and configurations are preferentially amplified. As they grow, they compete via interactions induced by the nonlinear terms in the equations which model the principal processes involved, and certain planforms win out. These are the patterns which are observed. They are universal in the sense that they depend only weakly on the details of the mechanisms involved in producing them. All patterns arising in systems with the symmetries of planar geometries (translation and rotation) display similar features. They consist of patches of the same planform, such as stripes with a preferred crest-to-crest length or, if the system has a broken up-down symmetry so that quadratic nonlinearities are important, superpositions thereof, which, with 120° relative angular orientations between the stripe directions, are hexagons.

Patterns on plants also arise from instabilities driven by a combination of the destabilization of uniform auxin concentrations and of the compressed annular generative region in the neighborhood of the plants SAM, as schematized in Fig. 13. The very center of the SAM (the tip of the plant shoot, Region 1 in Fig. 13) is a stem-cell region characterized by relatively low cell activity and division, but primordia appear in the generative region (Region 2) and continue to differentiate into mature organs (phylla) in Region 3.

In the growing shoot, some cells are displaced from the central region into the generative region where the cells in certain locations will initiate new leaf primordial forming spirals or whorls. The formation of leaf primordia consumes most of the generative region, which must be restored by displaced cells of the central region before the next cycle of leaf initiation. This so-called *plastochronic change* is essential to understanding the formation of phyllotactic patterns and distinguishes plant patterns from the other patterns we have discussed. In our model, we think of repeated regeneration of the generative region as an annulus-by-annulus generation process with the preferred pattern advancing as a front into a region in which certain instabilities are about to become manifest. An essential parameter diagrammed in Fig. 13 is the average radius R of the annular generative region. As a plant increases in size, R increases as well. There is also a second scenario (what we call the "sunflower scenario"), in which the oral primordia first form at the outer edge of the disk-like inflorescence meristem, and the generative zone and the pattern of initiating primordia propagates inwards. In this case, R decreases as the pattern progresses. In the first (respectively, second) scenario, the spiral families with the lowest (respectively, highest) Fibonacci numbers appear on the outside.

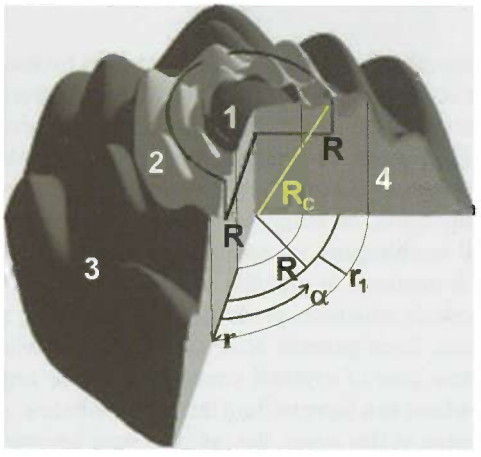

Figure 13. A schematic of the SAM, showing the annular generative region of active primordium generation (region 2) between a less active region at the center of the SAM (region 1) and a region of cell differentiation of no new primordium (region 3). We denote the average radius of the generative region by R.

The key point that we emphasize again and again about plant patterns is that they are laid down, not all at once as in most of the examples with planar geometry, but rather in repeated cycles of leaf initiation that are coordinated with repeated restoration cycles of the generative region. As the pattern is formed, the radius R of the generative region may change. The size of the primorida relative to the size of the central region, the duration of the plastochron (the time between the initiation of successive primordia), and the phyllotactic order may also change (Kelly & Cooke [22]). Although for simplicity we will refer in the following to changes in R, the important parameter is a ratio of R to the length scale of the pattern (distance between primordia). The pattern length scale may be most easily measured by the plastochrone ratio, which is the ratio from the apex to the second youngest primordium over the radius to the youngest primordium (Williams [45]).

Because of this way in which patterns are formed, the choice amongst all possible outcomes in any given generative annulus is heavily influenced by the pattern which has just been previously laid down in the neighboring annulus. Bias is not an unknown process in development. Cell differentiation turns stem cells into differentiated ones. It is this bias feature which allows Fibonacci-spiral patterns to be the preferred planform over the hexagonal lattices which are seen in most pattern-forming systems with planar geometries and broken up-down symmetries. Think of a landscape (physicists would call this a free-energy landscape) with lots of hollows (minima), some deeper than others, and place a ball (the starting position of the pattern) near one of the minima, as in Fig. 14. It will not necessarily roll into the deepest minimum, but rather into the local minimum in whose basin of attraction it initially lies. As the radius R of the generative annulus gradually changes, the energy landscape slowly evolves, and the minima move. If the change is slow enough, the pattern at the previous minimum will "roll" into the nearby minimum hole to which the previous minimum has evolved. What we find is that, as the radius R of the generative annulus changes, there is a continuous locus of new minima and, on this locus, the pattern will climb whatever Fibonacci-like sequence of spiral families it started on. Only in certain special circumstances will the ball (the pattern) roll into the deepest minimum, which, we have shown in [36], corresponds to a whorl pattern. Likewise, it takes a special perturbation to have the ball (the pattern) transfer from one Fibonacci sequence such as 2,3,5,8,13...) to another such as 3,2,5,7,12 ...). The reason is connected with the facts that (a) the loci of minima for each Fibonacci sequence changes continuously as R changes, (b) the loci of "whorl" minima do not change continuously with R, and (c) there are energy barriers between the loci of minima of the different Fibonacci sequences. Thus, it takes a substantial push to have the pattern change minima. The delineation of such cases with explanations for these nonsmooth changes, which often involve defects, is one of the many outstanding challenges for plant scientists.

This new approach, with which we have been most connected [28, 29, 30, 31, 35, 36, 37], attempts to build a model for phyllotaxis on the bases of the interconnected mechanisms of biochemistry and biomechanics. The ideas stem from two sources. The first proposed mechanism was pioneered by Paul Green and colleagues [13, 12, 8, 41] and was based on the idea that differential growth in the plant's tunica could lead to compressive stresses sufficiently large to cause buckling in the generative region. The idea was then that at certain stress maxima, biochemical reactions triggered by stress inhomogeneities and variation in the surface geometry would lead to the formation of phylla at these locations. The connection between stress and growth in biological tissue is a very important and largely still open challenge. The second mechanism is based on the work of the laboratories of Kuhlemeier [10, 32, 33, 39], Meyerowitz [21, 16, 14] and Traas [2] in the early 2000's. Reinhardt *et al.* [32, 33] had already shown that the presence and absence of the hormone auxin had a powerful effect on the stimulation or inhibition of the formation of primordia. The question was: how might variations in auxin concentration occur naturally so as to provide sites for new primordia? In equilibrium situations, nonuniformities in chemical concentrations are smoothed out by diffusion. What the laboratories of Kuhlemeier and Meyerowitz showed, however, was that in the vicinity of the SAM, the situation was not an equilibrium one. Excess auxin in one cell rela-

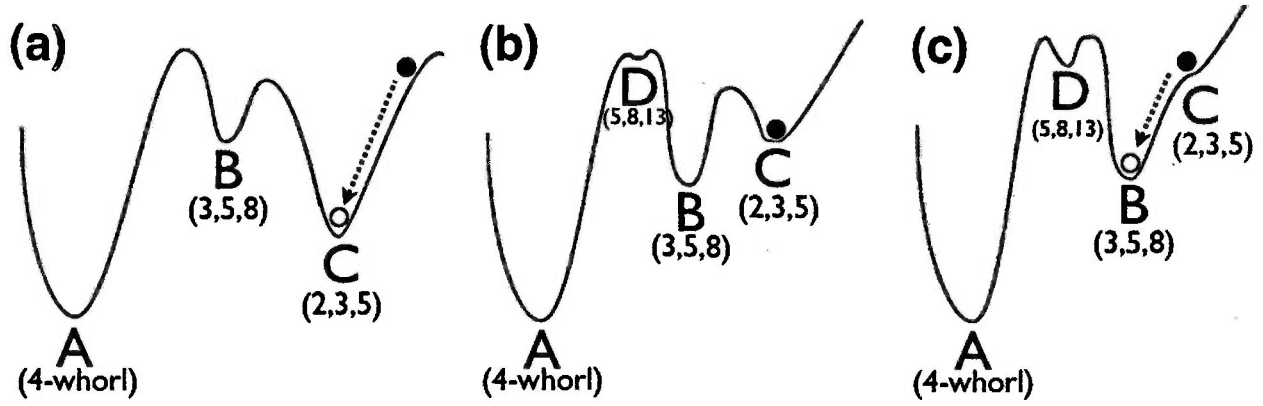

Figure 14. Above is a schematic of a changing energy landscape. A ball set loose in the energy landscape of panel (a) with local minima at A, B, and C, may fall into position C, although the global minimum is at A. The landscape changes (slowly) so that in panel (b) even the minimum at B is lower than the minimum at C, but without any external push, the ball stays at minimun C. As the landscape continues to evolve, C finally is the mere ghost of a minimum, and the ball falls to position B (still not a global minimum). In panel (b), a new minimum appears at D, and as the landscape continues to evolve, the ball may eventually fall into a succession of minima without ever landing in the global minimum.

tive to its neighbors triggered an action which sent a certain PIN1 protein from the cell interior to the cell walls where it oriented so as to pump auxin with its auxin gradient. This reverse diffusion effect, when sufficiently strong, can overcome ordinary diffusion and lead to instabilities and a natural quasiperiodic array of auxin concentration maxima and minima. This is precisely the ingredient one needs for preferential sites for primordium initiation.

In our work, we took advantage of the fact that the length scale $(2\pi/k_0)$ of the auxin concentration variation was many cell diameters and replaced a cell-by-cell analytical description of auxin concentration interactions developed by Jönsson, *et al.* [21] by a continuum model. For example, our SEM images of cacti show typical cell widths as 7μm, whereas a typical distance between primordia at initiation is about 100μm, a factor of about 15 difference. There is considerable advantage in going from a cell-to-cell model to a continuous model, as it allows us to make analytical progress rather than relying on large-scale simulations. It turns out that the resulting partial differential equation for the auxin concentration fluctuations has a canonical form associated with many pattern-forming systems. Near onset, namely near the value of the stress parameter which expressed the amount ϵ by which reverse diffusion exceeds ordinary diffusion, the equation takes the form:

$$\frac{\partial g}{\partial t} = (\varepsilon - (\Delta + k_0)^2)g + \text{nonlinear terms}$$

Further, since it is well known, but not at all well understood, that there is a strong coupling between stress and growth in living tissue, we included the mechanical stress fields so as to incorporate the ideas of Green *et al.* The growth strain g(**x**, t) resulting from fluctuations in auxin concentrations affects the stress field through the stress-strain relation. We modelled the effect of stress on growth by the simple idea that growth is induced when cells are under a tensile stress. We added a term proportional to the trace of the fluctuation stress tensor (the best measure of "pulling apart") to equation (1) for g. The coupled equations for the fluctuating surface deformation $w(\mathbf{x}, t)$ normal to the curved elastic shell which constitutes the plant's tunica and for the growth strain $g(\mathbf{x}, t)$ have very much the same form. For the buckling deformation $w(\mathbf{x}, t)$, the corresponding ϵ (ϵ_m) is the amount by which the compressive stress exceeds a critical threshold, and there is also a corresponding preferred wavelength $2\pi/k_{0,m}$. When the two preferred wavelengths k_0 and $k_{0,m}$ are nearly equal and and m are near zero, the combination of effects leads to an enhanced instability. We have shown that in this case, the positions of the auxin concentration maxima, where presumably the phylla are initiated can be very different from the surface morphology and lead to spiral-like behavior of the former and ridge-like behavior of the latter.

Key messages of our work are that, in certain circumstances, Fibonacci-spiral and whorl configurations are also a consequence of the solutions of pattern-forming PDEs. Moreover, all of the self-similar properties which are consistent both with observations and with the outcomes of discrete dynamical system algorithms continue to obtain. The PDEs contain more information and an invariant associated with the amplitudes of the modes which are dominant at any location. The role of the key parameter of the discrete dynamical system, the distance between radial values at which primordia are laid down, is taken by the radial distance R from the apex of the plant's growth stem at which the pattern is formed. As we have said, unlike planar patterns, plant patterns form annulus-by-annulus, and the presence of one configuration created at a different value of R in the neighboring annulus affects the outcome in the pattern-forming annulus. We can model the evolving pattern formation as a front through which the unstable unpatterned state is invaded by a patterned state whose configuration is slowing changing, depending on the current front location. Equivalently, when we write the dynamics in terms of active mode amplitudes, we can model the local formation as an evolving minimum of some energy functional which moves continuously through some appropriately chosen parameter space.

The strength of this second approach is that it is based upon actual physical and biochemical mechanisms experienced by the plant. Indeed, it is very evident in recent work in the Meyerowitz laboratory that mechanical stresses are nonuniform in the neighborhoods of emerging primordia. Moreover, the parameters in the model equations derive from quantities which can be measured.

The weakness of this approach is that the analysis uses a decomposition, the amplitude equations, for the fields g and w which is better suited to large domains and has to be interpreted as a frontal region in the pattern context.

The Role of Mathematics as a Unifying Perspective

Mathematics, like a good poem, strips away the superfluous and fuses the essentials into a kernel of truth as it reveals the universal themes hidden amidst the great complexities of life. For pattern descriptions, fields such as the auxin concentration fluctuation or the normal deformation of the plant tunica surface, are represented by combinations of periodic modes whose shapes are determined by analyzing the stability properties of the uniform states. The set of all deformations is then split into active and passive sets, the amplitudes of the latter being determined by algebraic relations with the amplitudes of the former. When one instability mechanism dominates the other, the active modes of one field are slaved to those of the other, and the two morphologies look similar. The active modes can often be represented as combinations of trigonometric cosines $a\cos(lr - m\alpha - \phi)$, where α is the amplitude of the mode, l m are the wave numbers which determine the orientation and wavelength of the mode, and ϕ is a phase constant. The parameters a, l, and m are known as order parameters, and starting from a model's partial differential equations, one can derive algebraic equations which they all satisfy. The reason that patterns from very different contexts look so similar is that the nature of these order-parameter equations depends more on the overall geometric symmetries shared by the different systems than on microscopic details. The algebraic order parameter equations for systems which share symmetries look very much the same.

The chosen values of the order parameters are those which minimize some cost functional. Such analyses give rise to algorithms, the outcomes of which are not dissimilar to the outcomes of the discrete algorithms based on the teleological explanation approach. We will not comment in depth here, but this coincidence would seem to suggest that there is a hitherto undiscovered connection between optimal packing algorithms and pattern-forming systems.

To give concrete examples, we look at fields produced by functions of the form

$$\omega(x,y) = a_1\cos(l_1x + m_1y) = a_2\cos(l_2x+m_2y)+a_3\cos(l_3x+m_3y),$$

for wave numbers l_j,m_j , plotted in the (x, y)-plane. If two amplitudes a_j are zero, so that, say, $\omega\ (x, y) = a_3\ \cos(l_3x+m_3y)$, one observes only ridges, as in Fig. 15(k,l). If, however, all amplitudes are positive and equal, a hexagonal pattern is observed Fig. 15 (a,b). The shape of the hexagons can be changed by either varying the wave vectors Fig. 15(a,b) or by making one Fig. 15(c,d) or two Fig. 15(e,f) amplitudes smaller. Simulations from this approach are given in Fig. 10, Fig. 16 and Fig. 17.

Open Challenges

There are many open and exciting questions which are best advanced by collaboration between observational, experimental, and theoretical scientists. We close with some questions and tasks for those working with or simply enjoying desert plants.

1. First and foremost is a question of importance for all biological tissue. How does elastic stress influence biochemical pathways and growth? For our model, this question is crucial for the coupling between the patterning due to auxin inhomogeneity and that due to elastic stress. Some recent reviews on the role of elastic stress in plant tissue include [4, 9, 15, 43].

2. What is the range of time scales for the formation of primordia in the generative region, and the length scales of the patterns? In particular, how do these scales in desert plants compare with other plants? The major point here is that models for phyllotactic mechanisms must address the range of biological spatio-temporal variation. Given the time for even a small molecule like auxin to diffuse across 1 mm or more of the surface of a sunflower inflorescence meristem, the establishment of local auxin minima does not seem to us to be able to account for the positions of new primordia on this. Of course, it may not be the regular diffusion time which is relevant. The relevant time is the time for the instability to grow, which depends on the difference between the destabilizing reverse diffusion and regular diffusion. It is clear that what is needed is a much better catalogue of all relevant times and parameters. To our knowledge, there is very little data available for desert plants, because it is only recently that the relevant time and length scales have been identified. In addition, it is clear from studies on Arabidopsis that plants are integrating stress fields and auxin gradients into coherent patterns of primordium positioning. How they do this and the relative importance of various mechanisms in a particular species is influenced by the time scales involved. Therefore, a clear identification of parameters to measure would be very valuable.

It would be useful if we could have direct measurements for desert plants to support or contradict the two mechanisms for primordium formation. First we might actually find ways to measure what the circumferential stress is for such plants in the generative regions and how it changes as we move away from this annulus. Second, we should be able to determine 1. if auxin plays any role on desert plants by repeating the Reinhardt, *et al.* experiment, and 2. if it is, to figure out how to measure the time scale required for any PIN1 protein in cells to feel an auxin gradient and respond by moving to the cell wall. This time scale would tell us if the observed primordium production rate is consistent with the picture that the reverse diffusion of auxin and its subsequent inhomogeneous distribution is the means by which primordia are first initiated in desert plants.

3. Transitions between pattern types on cacti have not been carefully cataloged or correlated with changes in the SAM, such as an increase in the mean radius R of the generative region. We have described transitions as occurring because parameters are changed enough so that certain minima disappear and the pattern is forced to fall into another minimum in the energy landscape. However, do random variation in parameters such as R ("noise") allow for patterns to jump barriers in the energy landscape independently of the disappearance or formation of new minima?

4. Once the morphological changes which accompany the maturation of primorida into phylla begin, the cells that have undergone those changes can only be transported by the overall growth of the plant. In most cases, that motion will be radially away from the center of the SAM. How do we include such behavior in the models in a natural way? For Hofmeister, the answer was simple:

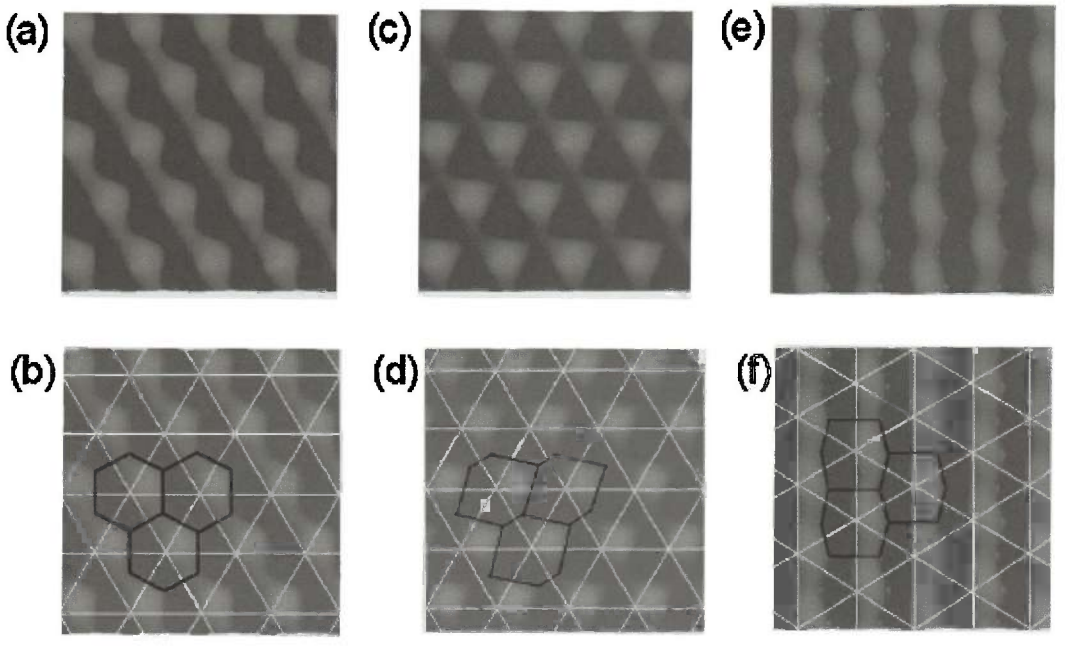

Figure 15. (a,b) $a_1 = a_2 = a_3 = 1$, $(l_1,m_1) = (-1,0)$, $(l_2,m_2) = ½, √3/2$, $l_3,m_3) = (½, -√3/2)$ (c.d) $a_1 = a_2 = 1$, $a_3 = 0.4$, (l_1,m_1) - (-1,0), $(l_2,m_2) = (½, √3/2)$, $(l_3,m_3) = (½,-√3/2)$, (e,f) a1 = 1, a2 = a3 = 0.3, $(l_1,m_1) = (-1,0)$, $(l_2,m_2) = (½, √3/2)$, $(l_2,m_3) = (½, -√3/2)$

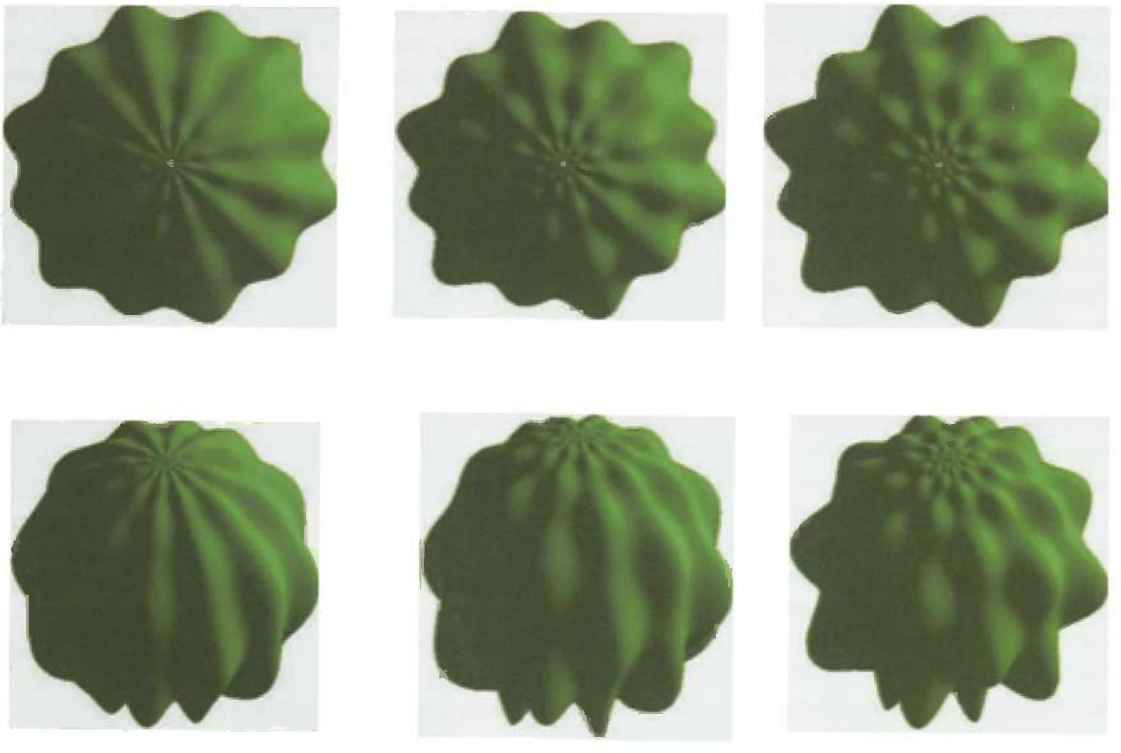

Figure 16. Cacti as the sums of periodic modes, from simulations of our model in (36).

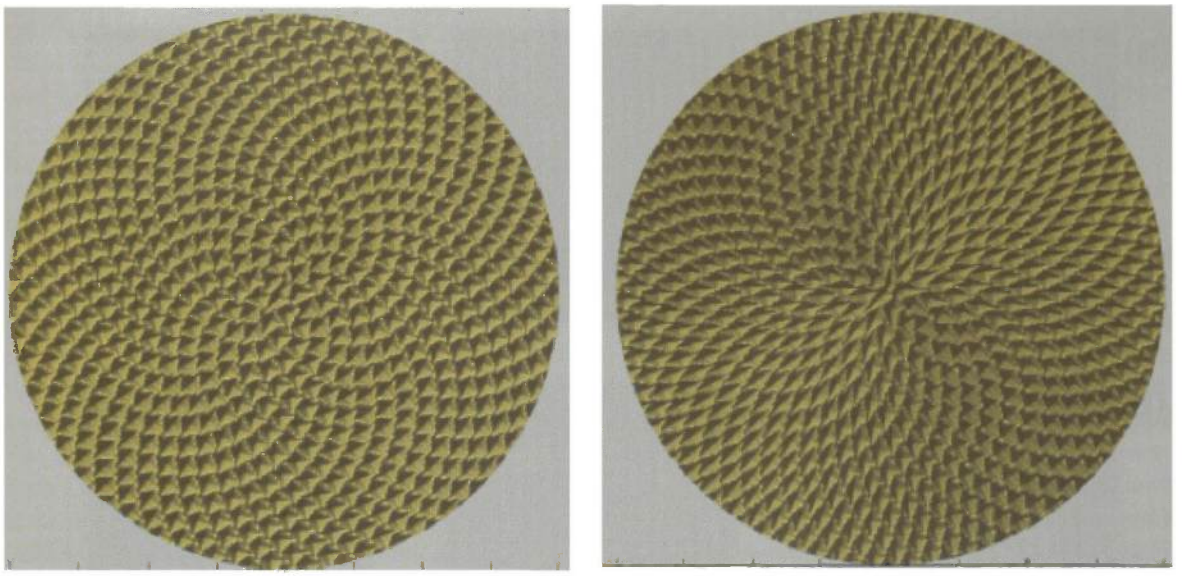

Figure 17. Sunflowers as the sums of periodic modes, simulations from our model [29,37].

he simply states that once a primordium has been laid down, its future radial position is never changed. For our pattern-formation approach, however, there is no a priori reason that the whole pattern behind the front at the generative region should not change. What are the natural processes connected with physics and chemistry that should be included in a model?

5. In models of epidermal ridge formation, one generally treats the epidermis as an elastic sheet undergoing compressive stresses because of the shrinking of the volar pads and the underlying dermis [24, 25]. But things can get more complicated, because it is known that the Merkel nerve cells connect with the pores along the epidermal ridges, and this it is not impossible that the underlying dermis plays more than a passive role. The same may be true for plants. There may be some pre-patterning behavior, or coupling behavior between the corpus and the tunica so that the former plays a more active role than being a source or sink for plant hormones.

6. In comparison to other plants, cactus primordia show less change in form as they differentiate and mature into phylla. The changes that do occur may provide some clues regarding the relationship between the processes involved in the initial primoridum formation and the eventual shape that the phylla take on. For example, look at the cacti in Fig. 18. All of these cacti show a hexagonal planform near their growth tips, but, away from the north pole, a ridge pattern begins to dominate over hexagons. Not having microscopic images of the pattern originally formed in the region of pattern formation, we cannot say what the full evolution of the pattern is after its original formation. Nevertheless, it is clear that the amplitude of one mode is increasing with respect to the other modes as material moves away from the growth tip. A similar situation is demonstrated by the paper cactus depicted in Fig. 19. Figs. 19(a,b) show a young paper cactus pad with a rhombus pattern; the two directions of largest amplitude are marked in Fig. 19(b). A rhombus pattern is, in our theory, produced by a sum

$$\omega(x, y) = a_1 \cos(l_1 x + m_1 y) + a_2 \cos(l_2 x + m_2 y) + a_3 \cos(l_3 x + m_3 y) + a_4 \cos(l_4 x + m_4 y) \quad (3)$$

of four periodic modes with amplitudes $a_2 \cong a_3 > a_1 \cong a_4$; the spirals marked in Fig. 19(b) correspond to the modes with amplitudes a_2, a_3. As the pad gets larger, as in Fig. 19(c,d), one notices that a third amplitude is getting larger, and, as the pad continues to get larger, a hexagonal pattern develops, as in Fig. 19(e,f). In terms of amplitudes, what has happened is that the amplitude a4 has increased, while a1 has decreased. Mature paper cactus pads show a hexagonal configuration, as in Fig. 19(g,h). This change from a rhombular to a hexagonal pattern occurs not at the growth tip, but after the pattern had moved out away from the growth tip. What mechanisms are involved in this change of the pattern? We suggest that a slight dominance of the purely radial deformation at the plant tip may induce changes in cell division and cellulose orientation so that this deformation grows further via feedback mechanisms as the patterned plant material differentiates.

7. Does the relevance of periodic mode summations to plant pattern topography extend to areola formation? Fig. 20(a) shows a cactus with a hexagonal planform; the three periodic deformations that (in our theory) produce it are marked. Notice that the areolas follow along the lines that would mark the directions of the fourth periodic deformation whose amplification would produce a rhombus pattern. In fact, near the very center of the plant the pattern is rhombic. The marked hexagonal configuration may then be a result of a change in an originally rhombular pattern, with evidence of the former presence of a fourth mode left by the areolas that formed. To determine the biological differences that lead to the differences between these two plants, one needs to know the form of the pattern as it develops in the generative region and the subsequent changes in the pattern as the plant grows.

8. What is the geometry of the cactus SAM? The geometry of the SAM may potentially be spherical, inverted spherical, or hyperbolic, as in Fig. 21. We expect this to influence the elastic stresses due to growth in the SAM, and therefore the pattern that forms. The importance of the geometry of the apex to the possible types of phyllotaxis has been noted in aquatic plants (Kelly and Cooke [22]). Does the geometry of the SAM account for different ex-

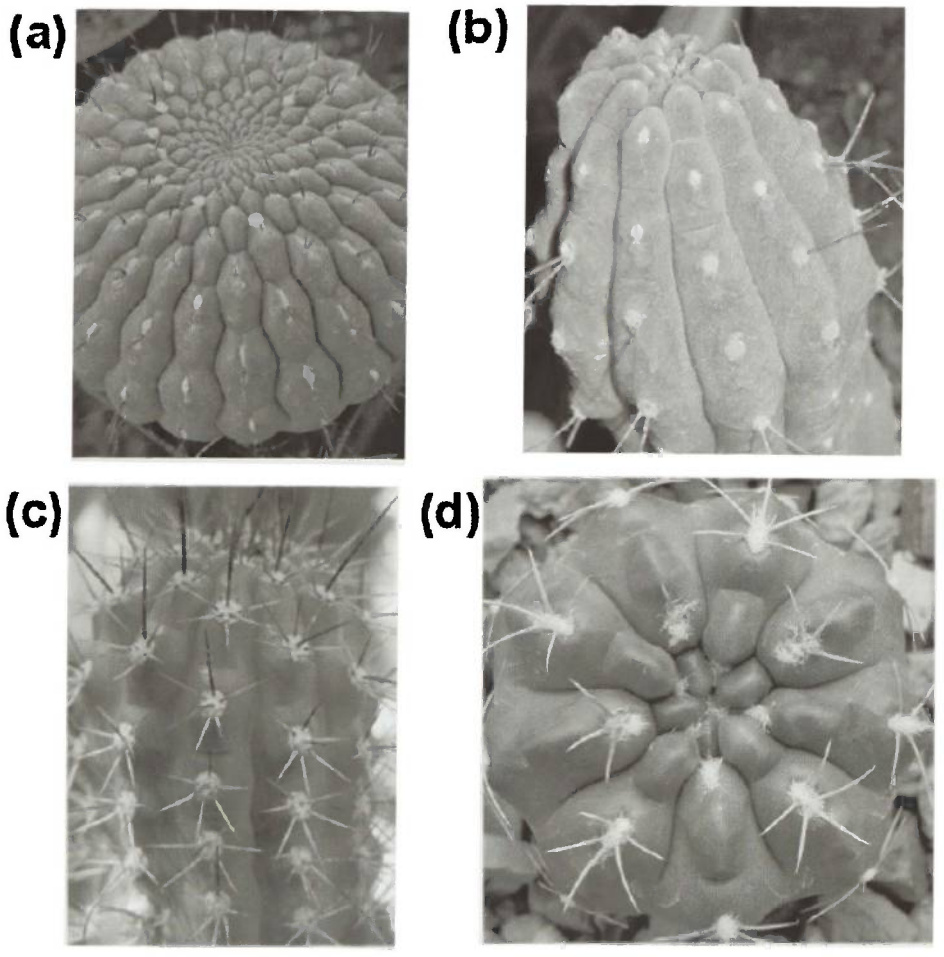

Figure 18. These cacti show hexagonal configurations near their north poles, but further from the north pole, the purely radial deformation becomes more dominant.

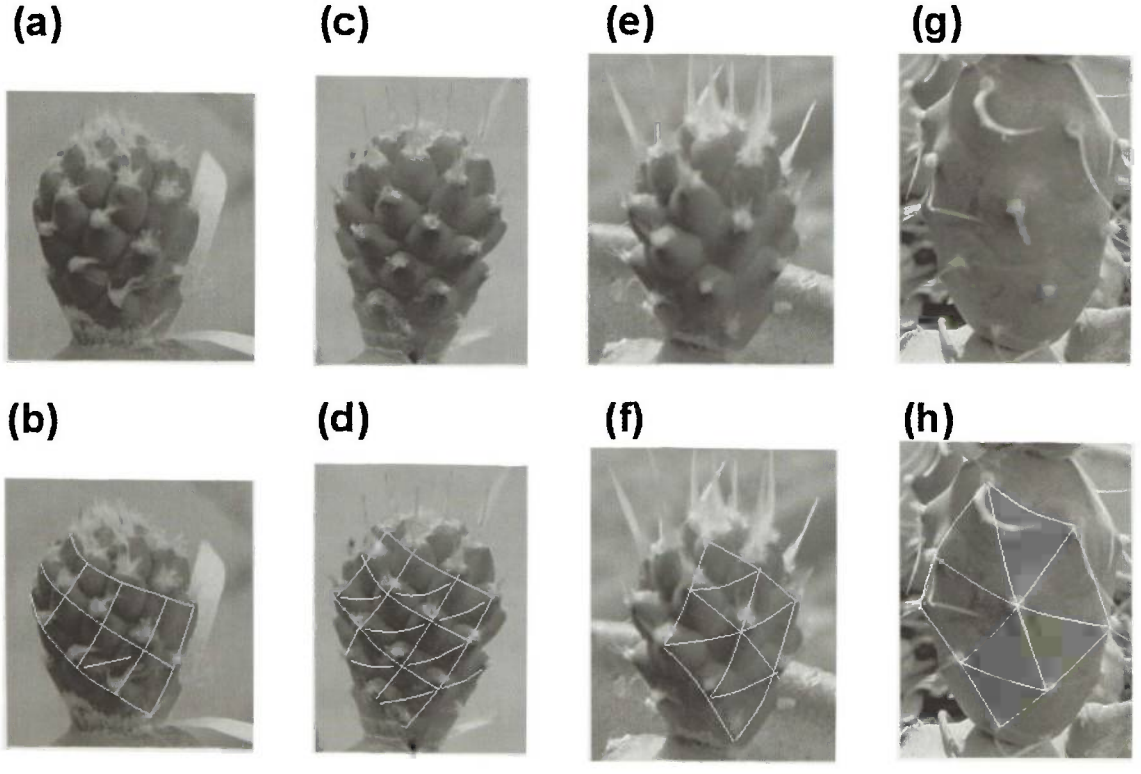

Figure 19. Rhombi (a,b), hexagons (g,h), and states in between (c,d,e,f) are seen on these pads of a paper cactus.

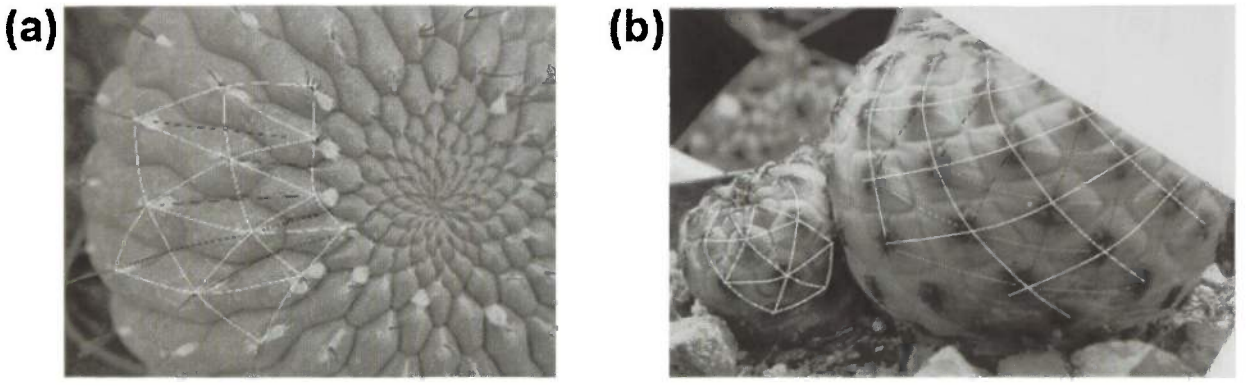

Figure 20. Diagrams of areole patterns that follow the periodic modes in our theoretical models.

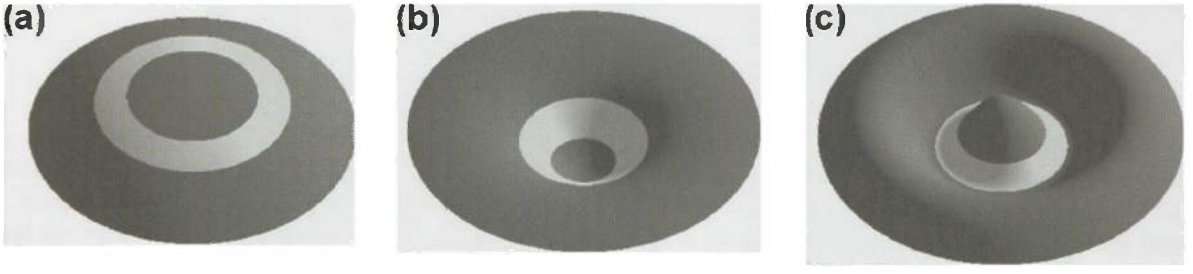

Figure 21. Possible geometries of a SAM: (a) spherical, (b) inverted spherical, or (c) hyperbolic.

pressions of whorled phyllotaxes in aquatic plants vs. cacti? In the emergent SAM's of aquatic plants, major changes in meristem dimensions do not affect the persistence of the whorled phyllotaxis, but the new whorls develop different numbers of primordia per whorl. Dimensional changes in those cacti capable of producing whorled phyllotaxes cause the phyllotaxis to switch back and forth between spiral and whorled.

Acknowledgements

We thank the National Science Foundation for grants DMS-0906024 to ACN and DMS-1022635 to PDS supporting these studies.

References

[1]Atela, P., S. Golée and S. Hotton. 2002. A dynamical system for plant pattern formation: Rigorous analysis. J. Nonlinear Sci. 12 (6), DOI 10.1007/s00332-002-0513-1.

[2] Barbier de Reuille, P., I. Bohn-Courseau, K. Ljung, H. Morin, N. Carraro, C. Godin, and J. Traas. 2006. Computer simulations reveal properties of the cell-cell signaling network at the shoot apex in Arabidopsis, Proc. Nat. Acad. Sci. 103, 1627-1632.

[3] Bierhorst, DW. 1959. Symmetry in equisetum American Journal of Botany 46: 170179.

[4] Braam, J. 2005. In touch: plant responses to mechanical stimuli. New Phytologist 165, 373-389.

[5] Busse, F. H. 1967. On the stability of two-dimensional convection in a layer heated from below. J. Math. Phys. 46, 140-150.

[6] Dosio, G. A. A., F. Tardieu, O. Turc. 2006. How does the meristem of sunflower capitulum cope with tissue expansion and floret initiation? A quantitative analysis. New Phytologist 170, 711-722.

[7] Douady, S. and Y. Couder. 1996a. Phyllotaxis as a dynamical self-organizing process, Part I: The spiral modes resulting from time-periodic iterations. J. Theor. Biol. 178, 255-274.

[8] Dumais, J. and C. R. Steele. 2000. New evidence for the role of mechanical forces in the shoot apical meristem. J. Plant Growth Regulation 19, 7-18.

[9] Dumais, J. 2007. Can mechanics control pattern formation in plants? Current Opinion in Plant Biology 10: 58-62.

[10] Fleming, A. J., S. McQueen-Mason, T. Mandel and C. Kuhlemeier. 1997. Induction of leaf primordia by the cell wall protein expansin. Science 276.

[11] Fujita, T. 1938. Statistische Untersuchung ueber die Zahl konjugierten Parastichen bei den schraubigen Organstellungen. Botanical Magazine 52: 425-433.

[12] Green, P. B. 1999. Expression of pattern in plants: Combining molecular and calculus-based paradigms, American J. of Botany 86.

[13] Green, P. B., C. S. Steele and S. C. Rennich. 1998. How plants produce pattern. A review and proposal that undulating field behavior is the mechanism. In: Jean, R. V. and D. Barabé (Eds.) Symmetry in Plants. World Scientific, Singapore, pp. 359-392.

[14] Hamant, O., M. G. Heisler, H. Jönsson, P. Krupinski, M. Uyttewaal, P. Bokov, F. Corson, P. Sahlin, A. Boudaoud, E. M. Meyerowitz, Y. Couder and J. Traas. 2008. Developmental patterning by mechanical signals in Arabidopsis. Science 322, 1650-1655.

[15] Hamant, O., J. Traas, J. 2010. The mechanics behind plant develoment. New Physiologist 185: 369-385.

[16] Heisler, M. G., H. Jönsson. 2006. Modeling auxin transport

and plant development. J. Plant Growth Regul., DOI: 10.1007/s00344-006-0066-x.
[17] Hernandez, L. H., P. B. Green. 1993. Transductions for the expression of structural pattern: Analysis in sunflower. The Plant Cell 5, 1725-1738.
[18] Hofmeister, W. 1868. Allegmeine Morphologie der Gewachse, Handbuch der Physiologischen. Botanik. Engelmann, Leipzig.
[19] Hoyle, R. 2006. Pattern Formation: An Introduction to Methods. Cambridge UP.
[20] Jean, R. 1994. Phyllotaxis Cambridge UP.
[21] Jönsson, H., M. G. Heisler, B. E. Shapiro, E. M. Meyerowitz, E. Mjölsness. 2006. An auxindriven polarized transport model for phyllotaxis. Proc. Nat. Acad. Sci. 103, 1633-1638.
[22] Kelly, W. J. and Cooke. 2003. Geometrical relationships specifying the phyllotactic patterns of aquatic plants. American Journal of Botany 90, 1131-1143.
[23] Kirchoff, B. K. Shape Matters: Hofmeister's rule, primordium shape, flower orientation. Int. J. Plant Sci. 164, 505-517.
[24] Kuecken, M. and A.C. Newell, A. C. 2004. A model for fingerprint formation. Europhysics Letters 68: 141-146.
[25] Kuecken, M. and A.C. Newell. 2005. Fingerprint formation. J. of Theoretical Biology 235: 71-83.
[26] Levitov, L. S. 1991. Energetic approach to phyllotaxis. Europhysics Letters 14, 533-9.
[27] McCully, M.E. and H.M. Dale. 1961. Variations in leaf number in Hippuris: a study of whorled phyllotaxis. Canadian Journal of Botany 39: 611625.
[28] Newell, A. C. and P. D. Shipman. 2005. Plants and Fibonacci. Journal of Statistical Physics 121, 937-968.
[29] Newell, A. C. and P. D. Shipman. 2008. A new invariant in plant phyllotaxis. Journal of Analysis and its Applications 6, 383-399.
[30] Newell, A. C., P. D. Shipman and Z. Sun. 2008. Phyllotaxis: Cooperation and competition between biomechanical and biochemical processes, J. Theor. Biol. 251, 421-439.
[31] Newell, A. C., P. D. Shipman, and Z. Sun. 2008. Phyllotaxis as an example of the symbiosis of mechanical forces and biochemical processes in living tissue. Plant Signaling and Behavior 8, 511-614.
[32] Reinhardt, D., T. Mande and C. Kuhlemeier, 2000. Auxin regulates the initiation and radial position of lateral organs. Plant Cell 12, 501-518.
[33] Reinhardt, D., E. R. Pesce, P. Stieger, T. Mandel, K. Baltensperger, M. Bennett, J. Traas, J. Friml and C. Kuhlemeier, 2003. Regulation of phyllotaxis by polar auxin transport. Nature 426, 255-260.
[34] Schwendener, S. 1909. Theorie der Blattstellungen. Sitzungsber. Akad. Wiss. Berl., 741-773.
[35] Shipman, P. D. and A. C. Newell. 2004. Phyllotactic patterns on plants. Phys. Rev. Lett 92 (16), 168102.
[36] Shipman, P. D. and A. C. Newell. 2005. Polygonal planforms and phyllotaxis on plants. J. Theor. Biol. 236, 154-197.
[37] Shipman, P. D. 2010. Discrete and continuous invariance in phyllotactic tilings. Physical Review E 81, id.031905.
[38] Shipman, P. D., M. Pennybacker, Z. Sun, and A.C. Newell. 2011. How universal are Fibonacci Patterns? European Physical Journal D 62(1), 5-17.
[39] Smith, R. S., S. Guyomarch, T. Mandel, D. Reinhardt, C. Kuhlemeier, and P. Prusinkiewicz. 2006. A plausible model of phyllotaxis. Proc. Nat. Acad. Sci. 103, 1301-1306.
[40] Snow, M. and R. Sno. 1952. Minimum areas and leaf determination, Proc. Roy. Soc. 545-566.
[41] Steele, C. R. 2000. Shell stability related to pattern formation in plants. J. Appl. Mech. 67, 237-247.
[42] Thompson, d'A. 1917. On Growth and Form. Cambridge UP.
[43] Uyttewaal, M., J. Traas and O. Hamant. 2009. Integrating physical stress, growth, and development. Curr. Opinion Plant Bio. 13, 1-7.
[44] van Iterson, G. 1907. Mathematische und microscopisch-anatomische Studien ueber Blattstellungen, nebst Betraschungen ueber den Schalenbau der Miloiolinen.
[45] Williams, R. F. 1975. The Shoot Apex and Leaf Growth. Cambridge UP.